Available online at www.sciencedirect.com
ScienceDirect
Geochimica et Cosmochimica Acta 70 (2006) 5855–5867
Geochimica
www.elsevier.com/locate/gca

Steady-state tracer dynamics in a lattice-automaton model of bioturbation

Daniel C. Reed [a,*], Katherine Huang [a], Bernard P. Boudreau [a], Filip J.R. Meysman [b]

[a] Department of Oceanography, Dalhousie University, 1355 Oxford Street, Halifax, Nova Scotia, Canada B3H 4J1
[b] Netherlands Institute of Ecology (NIOO-KNAW), Centre for Estuarine and Marine Ecology, Korringaweg 7, 4401 NT Yerseke, The Netherlands

Received 2 August 2005; accepted in revised form 27 March 2006

Abstract

The intensity of biogenic sediment mixing is often expressed as a ''biodiffusion coefficient'' (D_b), quantified by fitting a diffusive model of bioturbation to vertical profiles of particle-bound radioisotopes. The biodiffusion coefficient often exhibits a dependence on tracer half-life: short-lived radioisotopes (e.g. ^{234}Th) tend to yield notably larger D_b values than longer-lived radioisotopes (e.g. ^{210}Pb). It has been hypothesized that this is a result of differential mixing of tracers by particle-selective benthos. This study employs a lattice-automaton model of bioturbation to explore how steady-state tracers with different half-lives are mixed in typical marine settings. Every particle in the model is tagged with the same array of radioisotopes, so that all tracers experienced *exactly* the same degree of mixing. Two different estimates of the mixing intensity are calculated: a tracer-derived D_b, obtained in the standard way by fitting the biodiffusion model to resulting tracer profiles, and a particle-tracking D_b, derived from the statistics of particle movements. The latter provides a tracer-independent measure of mixing for use as a reference. Our simulations demonstrate that an apparent D_b tracer-dependence results from violating the underlying assumptions of the biodiffusion model. Breakdown of the model is rarely apparent from tracer profiles, emphasizing the need to evaluate the model's criteria from biological and ecological parameters, rather than relying on obvious indications of model breakdown, e.g., subsurface maxima. Simulations of various marine environments (coastal, slope, abyssal) suggest that the time scales of short-lived radioisotopes, such as ^{234}Th and ^{7}Be, are insufficient for the tracers to be used with the biodiffusion model. ^{210}Pb appears an appropriate tracer for abyssal sediments, while ^{210}Pb and ^{228}Th are suitable for slope and coastal sediments.

1. Introduction

The majority of Earth's surface is covered with water overlying sediments and most of these sediments are inhabited by benthic fauna. Sediment mixing caused by faunal activities, commonly termed bioturbation (Richter, 1952), impacts upon a wide range of sediment properties and processes. Modification of the physical structure of sediments by bioturbation affects their stability and erodibility (Yingst and Rhoads, 1978). Organism-mediated reworking of sediments obfuscates the geological record by destroying stratification, altering the apparent timing and intensity of events and consequently hindering our view of the past (Berger and Heath, 1968). Biological redistribution of chemical species, such as contaminants, influences chemical fluxes and, thus, exchange with the water column (Bosworth and Thibodeaux, 1990), and can initiate reactions that would otherwise be absent by providing transport mechanisms between chemically distinct zones (Aller and Rude, 1998). Therefore, the ability to provide an accurate description of benthic processes is frequently reliant upon a good quantitative measure of bioturbation.

Bioturbation consists of many varied modes of sediment transport. Mechanisms for displacing sediment include burrowing, construction and maintenance of dwellings, ingestion and subsequent egestion of sediment grains, infilling of abandoned living structures and ''ploughing'' of the sediment–water interface by epifauna. The opacity of sediments impedes direct observation of animal–sediment interactions, necessitating alternative methods of study.

* Corresponding author.
E-mail address: Daniel.Reed@dal.ca (D.C. Reed).

0016-7037/$ - see front matter © 2006 Published by Elsevier Inc.
doi:10.1016/j.gca.2006.03.026

The most common approach is to consider the vertical distribution of solid phase tracers, such as particle-bound radionuclides (e.g. ^{210}Pb, ^{234}Th) and introduced particles (e.g. luminophores, glass beads). Rather than attempting to quantify individual mixing events and specific modes of reworking, most bioturbation studies aim to determine a generic time-averaged measure of mixing intensity by fitting mathematical models to these vertical tracer profiles. By far the most popular model of bioturbation is the biodiffusion model, which assumes that Fick's laws of diffusion are applicable to bioturbation (Goldberg and Koide, 1962; Guinasso and Schink, 1975; Boudreau, 1986a). Fitting this model to tracer profiles furnishes a value for the "biodiffusion coefficient" (D_b), which characterises the intensity of mixing.

The biodiffusion model has the advantage of mathematical simplicity and the convenience of reducing a complex system to a single parameter. Furthermore, in practice, the diffusion analogy has proven to be a robust empirical model: radioisotope profiles in reworked sediments often show the exponentially decreasing depth-dependence predicted by the diffusion equation (e.g. Cochran, 1985; Stordal et al., 1985; Green et al., 2002). However, theoretical analysis has shown that in adopting a diffusive view of bioturbation, certain assumptions are made with regard to the length, frequency and symmetry of particle displacements (Boudreau, 1986a; Meysman et al., 2003c). Accordingly, the biodiffusion model has its limitations, and one should be cautious about violation of the underlying assumptions when deriving D_b values from tracer profiles.

Radioactive tracers of different half-lives are employed to examine bioturbation on different temporal and spatial scales, depending on the intensity of the mixing regime and sedimentation rate (Aller, 1982). A remarkable observation is that biodiffusion coefficients often exhibit a dependency on tracer half-life ($t_{1/2}$). That is, for exactly the same sediment, short-lived radioisotopes tend to yield larger D_b values than longer-lived radioisotopes (Smith et al., 1993, 1997; Turnewitsch et al., 2000). It has been hypothesized that the relationship is a consequence of "age-dependent" mixing: differential mixing of tracers due to their association with particles of different nutritional value (Smith et al., 1993). This theory asserts that short-lived tracers are chiefly associated with young and, therefore, labile particles. As a result, short-lived tracers are preferentially ingested by particle-selective benthos and consequently mixed at a greater rate than longer-lived tracers, which are predominantly associated with refractory material. If age-dependent mixing is indeed real, it poses significant difficulties for biogeochemical modelling since no unique mixing intensity can be assigned to all the solid constituents, as is the standard practice in current early diagenetic models (Boudreau, 1996; Meysman et al., 2003b).

This study employs a novel modelling approach to bioturbation to examine how steady-state tracers with different half-lives are mixed in typical marine settings. The model allows a tracer-independent D_b to be determined by tracking particle movements, thus providing a reference for tracer determined values. Our work reveals an alternative mechanism that can produce the observed relationship between D_b and $t_{1/2}$ in the *absence* of a differential mixing mechanism. That is to say, even when radioisotopes are exposed to exactly the same intensity of reworking, the trend persists.

2. Mechanistic modelling of bioturbation

While the biodiffusion model is certainly a useful tool, adopting a single parameter to represent the net community effect of bioturbation masks the mediators and modes of reworking. Alternatively stated, the model largely neglects biology—the very core of bioturbation, by definition—due to its one-size-fits-all approach. As a result, it is unclear how the multitude of animal–sediment interactions contribute to mixing and, consequently, how changes in community structure and faunal behaviour affect the mixing rate.

In an attempt to introduce biology to the biodiffusion coefficient, Wheatcroft et al. (1990) decomposed the biodiffusion coefficient into biologically relevant parameters, i.e., step length (the distance of particle movements) and rest period (the time between movements). This decomposition was developed from a random walk model assuming a constant step length and rest period estimated from published data (see Table 1 in Wheatcroft et al., 1990).

Random walk models are incredibly powerful, as they allow the stochastic behaviour of individual particles to be extrapolated into a deterministic description of bulk sediment transport (Wheatcroft et al., 1990; Meysman et al., 2003c). This is of great benefit in the analysis of bioturbation, as conventional tracer studies consider large populations of particles, whereas, in actuality, bioturbation acts of the level of individual particles, which are displaced in discrete mixing events. Therefore, random walk models effectively allow a critical mechanistic link between bioturbation and tracer distributions to be established. Various random walk models representing different mixing mechanisms can be constructed by making specific assumptions regarding the frequency and length of particle displacements. Owing to the variability in particle movements, probability density functions are used to represent the frequency and length of particle displacements, as opposed to constants. Consequently, it is necessary to be able to define such functions to reflect faunal mixing behaviour. Ideally, the required information regarding particle motion should be achieved by tracking individual particles under natural conditions. Unfortunately, this is not feasible with present day technology. The lack of *in situ* or laboratory data at the individual particle level provides motivation for the development of alternative approaches. With this in mind, the Lattice-Automaton Bioturbation Simulator (LABS) was advanced by Choi et al. (2002) to provide the ability to collect information on bioturbation *simultaneously* on both the level of individual particles and populations of particles, thus, affording faunal behaviour and biological

parameters to be directly related to sediment reworking rates.

LABS is a computational model comprising a two-dimensional sediment–water lattice (in the vertical aspect) inhabited by automatous entities. Stochastic and deterministic rules govern the behaviour of these ''automatons'' to mimic real fauna, passing through the sediment–water matrix, displacing particles by burrowing, feeding, etc., and thus mixing the sediment. LABS is not an alternative to inverse models, which interpret tracer profiles; nor is it an alternative to random walk models, which consider the stochastic behaviour of individual particles. This is because LABS does not *analyse* data, but *generates* synthetic data to which inverse and random walk models can be applied. In a sense, LABS relates to a natural sediment as a flight simulator relates to an actual aeroplane. As such, LABS is specifically designed as a learning tool to increase our understanding of bioturbation. A first possibility is to examine the implications of different faunal characteristics and behaviour. Parameters such as ingestion rates, organism dimensions, faunal densities, and community structure can be varied, and their effect on tracer profiles readily deduced. In this way, Boudreau et al. (2001) employed LABS to examine the influence of various biological parameters on biodiffusion coefficients determined from ^{210}Pb tracer profiles.

Here, LABS is used to examine the limitations of current modelling theory. The significant advantage offered by LABS is that it allows mixing intensity to be determined in two independent ways. First, all particles in the model can be tracked, allowing the mixing intensity to be determined solely from the statistics of particle displacements. This so-called particle-tracking D_b is derived from random walk models of individual particle movements and is therefore tracer-independent. Second, within LABS, sediment particles can be assigned attributes such as chemical properties, allowing them to be tagged with radioisotopes. Tracer profiles are achieved by averaging the activity of the particles in lateral ''slices'' of the sediment matrix. Subsequently, a so-called tracer-derived D_b can be determined in the usual manner, by fitting the biodiffusion model to these vertical tracer profiles.

A brief description of LABS follows; a detailed description can be found in Choi et al. (2002).

3. Lattice-automaton bioturbation simulator

LABS is a two-dimensional matrix of cells that take one of three forms: (1) porewater, (2) sediment ''particles'', (3) organism. As modelling individual sediment grains is impractical, LABS instead considers quasi-particles approximately the size of sediment parcels handled by benthic fauna. Initially, particles are distributed randomly throughout the matrix at a user-set porosity. A sediment–water interface is defined, above which exists a small water column. The dimensions of the matrix and depth of the mixed layer are also chosen by the modeller. Organisms with user-specified parameters (e.g. size, ingestion rate, abundance) are then introduced to the matrix, behaving in a manner defined to imitate benthic organisms. Organisms are made up of a collection of adjacent cells that move in unison according to prescribed rules. The animals' rules are both deterministic and probabilistic, acknowledging the stochastic nature of biology. This is an important aspect of LABS, as it allows the variability of bioturbation to be considered—something that has largely been ignored in past models of bioturbation. Moreover, probability-based rules coupled with a two-dimensional domain allows the development of heterogeneities, like those observed in nature.

The automatons used in this study represent subsurface deposit-feeders, i.e., mobile worms that burrow through the mixed layer ingesting and egesting particles as they go. They proceed through the lattice by parting the sediment grains immediately in their path from the centre of the burrow outwards, in a similar fashion to the fracture-based burrowing mechanism recently advanced by Dorgan et al. (2005). The result is a porewater filled burrow the width of the organism with a compacted lining. Over time, these burrows decay and collapse. Generally, the automatons select burrowing directions randomly, producing a random path through the matrix. There are, however, rules in place to prevent the automatons from burrowing below the mixed layer, into the water column or into themselves. Depth-dependent burrowing rules can be implemented, for example, a linearly increasing reluctance to venture deeper into the sediment. In this scenario, the probability of burrowing downwards is zero at the base of the mixed layer and increases linearly until it is as equally likely as any other direction at the sediment–water interface. (The implications of such a rule are discussed in Section 6.4.) As they progress through the sediment matrix, the automatons ingest particles at a prescribed ingestion rate and defecate previously ingested particles. Owing to the random nature of burrowing, ingestion and defecation are not restricted to specific regions of the sediment.

Particles are introduced to simulations by sedimentation from the water column onto the sediment–water interface. Porosity-based algorithms are used to simulate compaction, decay of animal burrows and to maintain the sediment–water interface. Originally written in FORTRAN 90 (Choi et al., 2002), LABS has been recast in an object-oriented design and coded in C++. This design facilitates maintenance and development of the code, such as addition of new functional groups of organisms (Meysman et al., 2003a). Currently, four functional groups exist in the model: subsurface deposit-feeders (used in this study), head-down deposit-feeders, J-tube deposit-feeders and burrow-and-fill mixers.

4. Quantifying mixing intensity: two alternative approaches

4.1. Tracer-derived D_b

One way of estimating the intensity of bioturbation is by fitting the biodiffusion model to vertical tracer profiles and

determining a corresponding D_b value. D_b as derived from tracer profiles is denoted D_b^t hereafter. When considering steady-state particle-bound radioisotopes, the one-dimensional biodiffusion model can take the form,

$$\frac{\partial C}{\partial t} = D_b^t \frac{\partial^2 C}{\partial x^2} - \omega \frac{\partial C}{\partial x} - \lambda C = 0 \tag{1}$$

where C is the tracer activity, x is depth with the sediment–water interface as the origin, t is time, D_b^t is the biodiffusion coefficient, ω is the sedimentation rate and λ is the tracer's decay constant. This form of the biodiffusion model assumes constant porosity, rate of burial and bioturbation with depth. Solution of Eq. (1) requires two boundary conditions, which are typically taken as,

$$C(0) = C_0 \tag{2}$$

$$\lim_{x\to\infty} \frac{\mathrm{d}C}{\mathrm{d}x} = 0 \tag{3}$$

Solving Eq. (1) with these boundary conditions gives,

$$C(x) = C_0 \mathrm{e}^{-\frac{x}{x_t}} \tag{4}$$

where x_t is the characteristic length scale of the tracer or "e-folding distance", and is defined as,

$$x_t = \frac{2D_b^t}{-\omega + \sqrt{\omega^2 + 4D_b^t\lambda}} \tag{5}$$

(Boudreau, 1997). When D_b^t, λ and ω are all positive constants, x_t is also positive and, therefore, $C(x)$ decays with increasing depth. Eq. (4) is fit to tracer profiles using a nonlinear least-squares method to determine the value of x_t and then D_b^t using,

$$D_b^t = x_t(\lambda x_t - \omega) \tag{6}$$

as all other parameters are known.

4.2. Particle-tracking D_b

An alternative approach to quantifying the intensity of mixing is by considering the motion of individual particles. Bioturbation activities, such as burrowing or infilling of living structures, displace particles to new positions in the sediment, where they remain until the next bioturbation event. Thus, sediment particles experience bioturbation as a series of displacements (or steps) and rest periods (Wheatcroft et al., 1990). In reality, step lengths and rest periods will show considerable variability due to the variety of organisms present and mixing modes at work. To account for this variability, one can adopt a stochastic view of particle movement, where particle displacements are considered sufficiently erratic that they can be modelled as stochastic variables. Accordingly, step lengths (L) and rest periods (T) are represented by appropriate probability density functions, $\vartheta(l)$ and $\phi(t)$, respectively. The probability of a rest period in the interval (t, $t + \mathrm{d}t$) is thus given by,

$$P(t < T < t + \mathrm{d}t) = \phi(t)\,\mathrm{d}t \tag{7}$$

The average period between two particle displacements is the mean of the probability density function:

$$\tau = \int_0^\infty t\phi(t)\,\mathrm{d}t \tag{8}$$

Similarly, the probability of a step length in the interval (l, $l + \mathrm{d}l$) is,

$$P(l < L < l + \mathrm{d}l) = \vartheta(l)\,\mathrm{d}l \tag{9}$$

The average step length (or drift) is therefore,

$$\mu = \int_{-\infty}^\infty l\vartheta(l)\,\mathrm{d}l \tag{10}$$

If the step length probability density function is symmetric, i.e., the motion of particles is isotropic, the mean displacement is zero. A characteristic length scale of particle movements is achieved by considering the variance, or the second central moment, of the step length distribution, i.e.,

$$\sigma^2 = \int_{-\infty}^\infty (l-\mu)^2\vartheta(l)\,\mathrm{d}l \tag{11}$$

Combining the two probability density functions provides the probability of finding a particle in the interval (l, $l + \mathrm{d}l$) at some time within (t, $t + \mathrm{d}t$), given that the particle was initially at the origin:

$$\Psi(l,t)\mathrm{d}l\mathrm{d}t = \vartheta(l)\phi(t)\mathrm{d}l\mathrm{d}t \tag{12}$$

Eq. (12) forms the basis of continuous-time random walks (Hughes, 1995; Metzler and Klafter, 2000). This probablistic model of a single particle's behaviour can be expanded into a deterministic description of bulk sediment transport by taking the so-called continuum limit. One can prove that in the long-time limit (i.e. after a sufficient number of bioturbation events), a continuous-time random walk always converges to the diffusion equation (Hughes, 1995)

$$\frac{\partial C}{\partial t} = D_b^p \frac{\partial^2 C}{\partial x^2} - \omega_b^p \frac{\partial C}{\partial x} \tag{13}$$

where the bioadvective velocity is defined as,

$$\omega_b^p = \frac{\mu}{\tau} \tag{14}$$

and the biodiffusion coefficient is given by,

$$D_b^p = \frac{\sigma^2}{2\tau} \tag{15}$$

This D_b^p value provides our alternative estimate for the mixing intensity and is referred to hereafter as the particle-tracking D_b.

Note that both ω_b^p and D_b^p are obtained solely from observations at the particle level and, therefore, particle-tracking does not impose a mixing model. In other words, these mixing parameters can be obtained from LABS regardless of whether tracer distributions are justifiably described by the biodiffusion model or not. When mixing is not diffusive, Eq. (15) still provides a measure of mixing intensity. By tracking the motion of individual particles, we can construct two frequency distributions: one for the

observed step lengths and one for the observed rest periods. These frequency distributions are then equated to the step length and rest period probability density functions, from which the required statistics are calculated by means of Eqs. (8), (10) and (11). In this way, a tracer-independent measure of mixing can be determined.

5. Multiple tracer simulation experiments

5.1. Preliminary results

To gain insight into tracer-dependent mixing, initial experiments were conducted using LABS, where every particle in the matrix was tagged with the same four commonly used radioisotopes (^{234}Th, ^{7}Be, ^{228}Th, ^{210}Pb; Table 1). As a result, all tracers experienced *exactly* the same degree of mixing. The initial distribution of tracers in the sediment matrix is produced by burial and decay alone and particles introduced to the lattice by sedimentation have unit activity. An array of commonly used tracers was used in these initial simulations so a general comparison could be made with published field observations. Unfortunately, lack of multiple tracer D_b data accompanied by *detailed* biological and ecological data for specific benthic communities precludes a site-specific comparison of field data and model output. However, use of "typical" parameters as model input allows a broad comparison to be made between model predictions and field observations. The model was "spun-up" for five times the half-life of the longest-lived tracer (i.e., $5 \times 22.3 \approx 112$ years) before data was harvested, to exclude any transient effects. Following this period, profiles for each tracer were output yearly for 100 years and from these profiles a value for D_b^t was determined.

In the preliminary model runs, the model's population consisted of burrowing subsurface deposit-feeding worms comparable to *Capitella* spp. in terms of size (2 cm × 0.2 cm; e.g. Grassle and Grassle, 1974), gut-to-body ratio (0.18; Penry and Jumars, 1990) and ingestion rate (50 mg d^{-1}). A specific ingestion rate of 8–10 mg sed mg^{-1} body wt d^{-1} for *Capitella capitata* (Forbes, 1984, as cited by Lopez and Levinton, 1987) and body weights of 3–12 mg (Grassle and Grassle, 1976) give a range of 24–120 mg daily, as smallest body sizes correspond to the lowest ingestion rates and *vice versa* (Méndez et al., 2001). The modelled organisms are mobile subsurface deposit-feeders and not sedentary, conveyor-belt or head-down deposit-feeders. Organism burrowing rate was set at 20 cm d^{-1} (cf. Caron et al., 1996) and faunal density at 1000 ind m^{-2}. Incidentally, these parameters mean that ingested particles pass through the gut at a slower rate than the organism burrows. Particles are, therefore, carried in the gut for a distance before being deposited. Clearly, the distance a particle is moved is highly variable depending on the path chosen by the organism immediately after ingestion.

The environmental parameters were chosen to represent a fairly typical marine sediment setting. The initial porosity was set to a uniform 0.8 throughout the sediment matrix. The sedimentation rate was set at 0.1 cm y^{-1} (e.g. a continental margin, Berner, 1980), while the mixed layer depth was chosen as the global average of 10 cm (Boudreau, 1994). Sedimentation occurred at a steady rate, as episodic burial influences tracer determined D_b values (Boudreau, 1986a).

Fig. 1 shows an example of a D_b^t time series from a LABS simulation. In this figure, D_b^t exhibits a notable tracer-dependence: short-lived tracers produced larger, more variable values relative to longer-lived tracers. ^{234}Th furnishes D_b^t values 1–2 orders of magnitude greater than ^{210}Pb, as observed in field studies (Smith et al., 1993, 1997; Turnewitsch et al., 2000). Furthermore, D_b^t values achieved for the various tracers are comparable to those observed in the field (e.g. Turnewitsch et al., 2000). It is worth emphasising that the model was in no way manipulated in an attempt to replicate the trends or values observed in nature. Reasonable parameters were used as model input and the relationship between D_b^t and $t_{1/2}$ was immediately apparent in the model output. In LABS, the trend is clearly not a manifestation of differential mixing of tracers, as no particle preferences were imposed on the automatons. Besides which, every particle was tagged with

Table 1
Commonly used steady-state particle-bound radioisotope tracers

Radioisotope	Half-life
^{234}Th	24.1 days
^{7}Be	53.3 days
^{228}Th	1.9 years
^{210}Pb	22.3 years

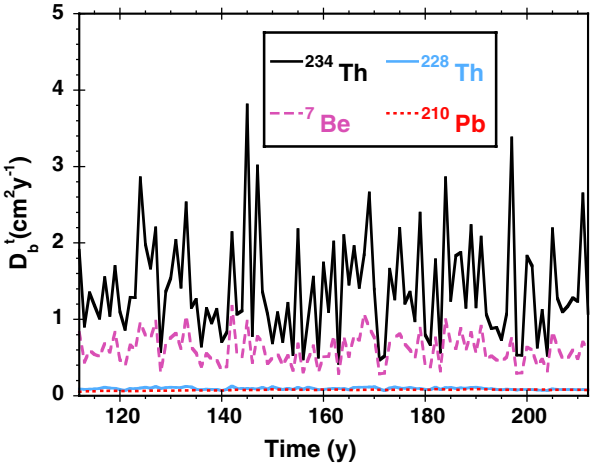

Fig. 1. A tracer-derived mixing coefficient (D_b^t) time series from LABS for four commonly used tracers: ^{234}Th ($t_{1/2} = 24.1$ d; solid black line), ^{7}Be ($t_{1/2} = 53.3$ d; dashed pink line), ^{228}Th ($t_{1/2} = 1.9$ y; solid blue line), ^{210}Pb ($t_{1/2} = 22.3$ y; dotted red line). The model population consisted of deposit-feeding worms 2 × 0.2 cm in size with a gut-to-body ratio of 0.18, ingestion rate of 50 mg d^{-1} and burrowing rate of 20 cm d^{-1}. The faunal density was 1000 ind m^{-2} and sedimentation rate 0.1 cm y^{-1}. Data were output yearly for 100 years.

the same array of tracers in order that all tracers experience an identical amount of mixing.

5.2. Further results

A second series of simulations were undertaken using multiple hypothetical radioisotopes with half-lives spanning several orders of magnitude. In these simulations, both tracer-derived and particle-tracking D_b values were determined using the procedures detailed in Section 4. In addition, the environmental conditions were varied to represent "typical" parameters for three marine regions: coastal, slope and abyssal (Table 2). The aim was to see if the previously observed trend was apparent in these marine settings and to gain a fuller view of $D_b^t(t_{1/2})$. The three scenarios used the same porosity and mixed layer depth as in the preliminary simulations, but differed in sedimentation velocity (Table 2). In the case of very low sedimentation rates, such as simulations of the deep-sea, insufficient tracer is supplied to LABS to produce profiles, owing to the small number of new particles being introduced. To overcome this problem without increasing advection in the system, the sediment–water interface is regularly "painted" with tracer (i.e. particles at the interface are set to unit activity). This means that tracer can be introduced by animals mixing tracer downwards. To enable comparison between the simulations, the sediment population in all scenarios consisted of the same type of organism, that is, subsurface deposit-feeding worms. The animals' dimensions, ingestion rate, burrowing rate and gut-to-body ratio were the same as used in the initial simulations; however, the faunal density was varied to reflect the decrease in mixing intensity with water depth (Table 2) (Middelburg et al., 1997).

Model output from all of these simulations show trends similar to the preliminary model runs, that is, an increase in D_b^t with decreasing $t_{1/2}$ (Fig. 2). D_b^t approaches D_b^p as $t_{1/2}$ increases, although the point at which these values deviate differs for the simulations (Fig. 2). Variability in D_b^t can also be seen to be a function of tracer half-life (Fig. 3). There are other prominent features to note in some of the simulations. Output from the coastal simulation shows D_b^t values decreasing (as $t_{1/2}$ increases) to a local minimum, after which D_b^t increases (Fig. 2c). Also, D_b^t values appear to drop below D_b^p during the slope simulation (Fig. 2b). The former can be shown to be an artifact resulting from the artificial lower boundary condition imposed in LABS, while the latter is due to spatial variability in D_b^t. The subsequent section contains a detailed discussion of these issues.

Table 2
Sedimentation rates and faunal densities used to simulate marine regions

Setting	ω (cm y^{-1})	ρ_{worms} (ind m^{-2})
Coastal	0.5	1×10^4
Slope	0.1	5×10^3
Abyssal	0.01	1×10^3

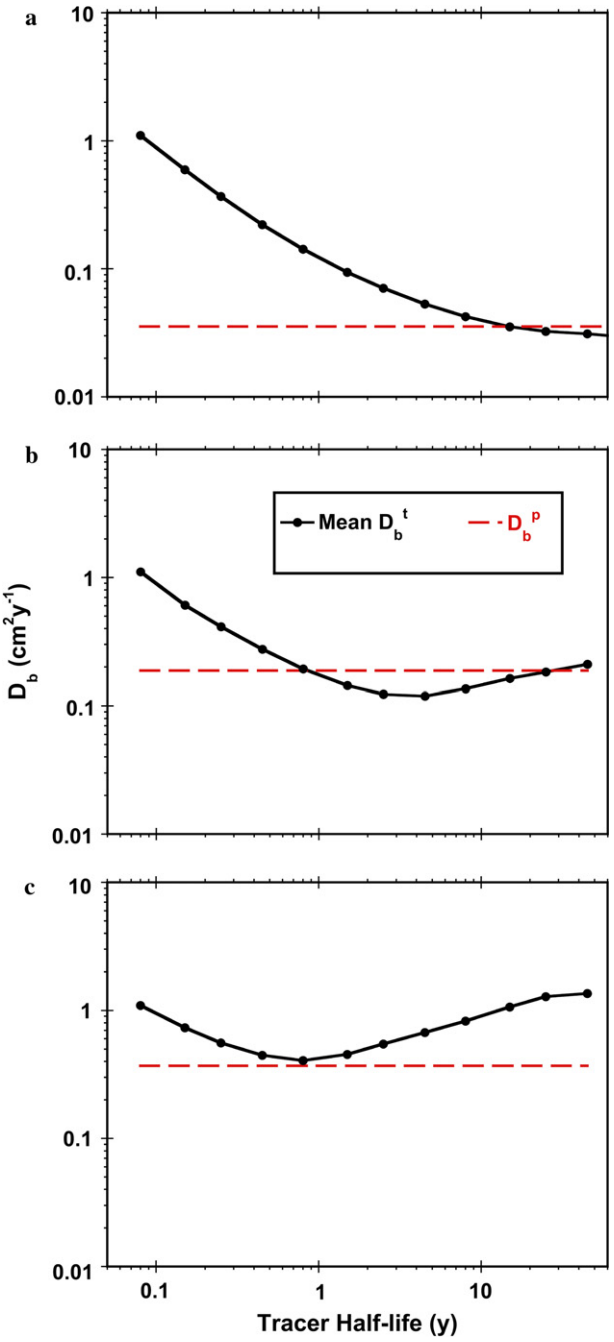

Fig. 2. The mean tracer-derived mixing coefficient (D_b^t; solid line) and particle-tracking mixing coefficient (D_b^p; dashed line) from LABS versus tracer half-life ($t_{1/2}$) for the (a) abyssal, (b) slope and (c) coastal parameter sets.

6. Discussion

6.1. Observation and mixing scales

An alternative way of considering the model output presented in Fig. 2 is in terms of scales. To this end, one can make a distinction between the spatial and temporal scales of observation, obtained by fitting the biodiffusion model to tracer profiles, and the spatial and temporal scales of

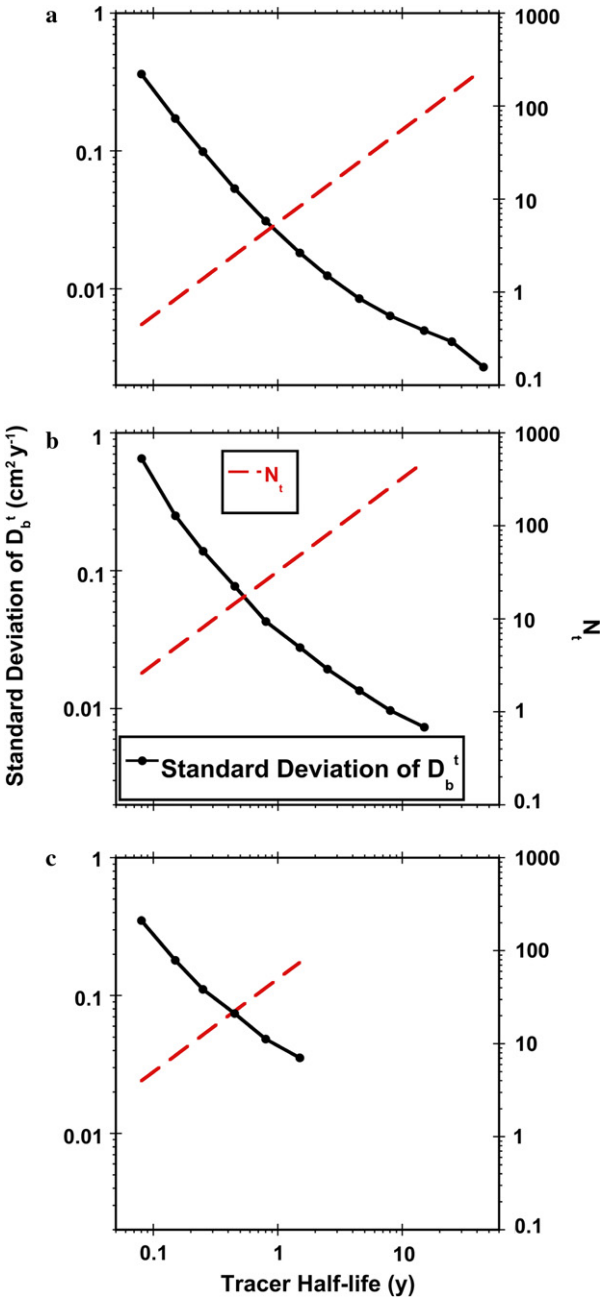

Fig. 3. The standard deviation of tracer-derived mixing coefficient (solid line), and average number of mixing events experienced by a radioisotope before decaying (N_t; dashed line) versus tracer half-life ($t_{1/2}$) for the (a) abyssal, (b) slope and (c) coastal parameter sets.

mixing, obtained from particle-tracking. As noted earlier, the tracer length scale can be represented as the e-folding distance of the profile, x_t. Assuming negligible burial to simplify the argument,

$$x_t = \sqrt{\frac{D_b^t}{\lambda}} \tag{16}$$

Eq. (16) shows that greater mixing intensities correspond to greater tracer length scales, i.e., deeper penetration of the tracer into the sediment. Similarly, the characteristic time scale of a radioisotope, t_t, is simply the inverse of its decay constant:

$$t_t = \frac{1}{\lambda} \tag{17}$$

These tracer scales can now be compared to the characteristic scales of mixing, as obtained from particle-tracking in LABS. As discussed in Section 4.2, the spatial and temporal scales of mixing, σ and τ, are obtained as the standard deviation of the step length distribution (Eq. 11) and the mean of the waiting time distribution (Eq. 8), respectively. σ and τ can be combined to obtain an estimate of mixing intensity, D_b^p (Eq. 15). When particle displacements are observed over a sufficiently long period of time, D_b^t will be in agreement with D_b^p. Accordingly, the tracer length scale, x_t, will agree with the predicted tracer length scale, x_p, where,

$$x_p = \sqrt{\frac{D_b^p}{\lambda}} \tag{18}$$

However, when observed over short time scales, such as for short-lived radioisotopes, the two independent estimates of the mixing intensity, D_b^t and D_b^p, may deviate from one another.

6.2. Comparison of scales

Random walk theory asserts that the biodiffusion model only becomes a valid approximation of a random walk when the time scale over which bioturbation is observed is much larger than the average time between two bioturbation events (Boudreau, 1986a; Hughes, 1995; Meysman et al., 2003c). Formally stated,

$$\tau \ll t_t \tag{19}$$

To examine this criterion, a dimensionless number is introduced representing the average number of times a particle is displaced before decaying:

$$N_t = \frac{t_t}{\tau} \tag{20}$$

For D_b^t to be a true representation of mixing, the tracer needs to experience a sufficient number of mixing events before decaying, e.g., $D_b^t \approx D_b^p$ when $N_t > 25$ Boudreau, 1986a. In this case, the observed tracer length scale will be,

$$x_t = \sqrt{\frac{D_b^t}{\lambda}} \approx \sqrt{\frac{D_b^p}{\lambda}} = \sqrt{\frac{\sigma^2}{2\tau\lambda}} = \sigma\sqrt{\frac{t_t}{2\tau}} = \sigma\sqrt{0.5N_t} \tag{21}$$

Eq. (21) predicts $x_t < \sigma$ when $N_t < 2$. However, this cannot occur, as σ represents a minimal depth at which tracer will always be found. That is to say, $x_t \geqslant \sigma$ regardless of N_t. The restriction on tracer length scale imposed by mixing length scale implies that when insufficient mixing events have been experienced, Eq. (21) will no longer be valid. Accordingly, the tracer length scale will be greater than anticipated ($x_t > \sigma\sqrt{0.5N_t}$) and the tracer derived mixing coefficient will be too large ($D_b^t > D_b^p$). Fig. 4 shows that

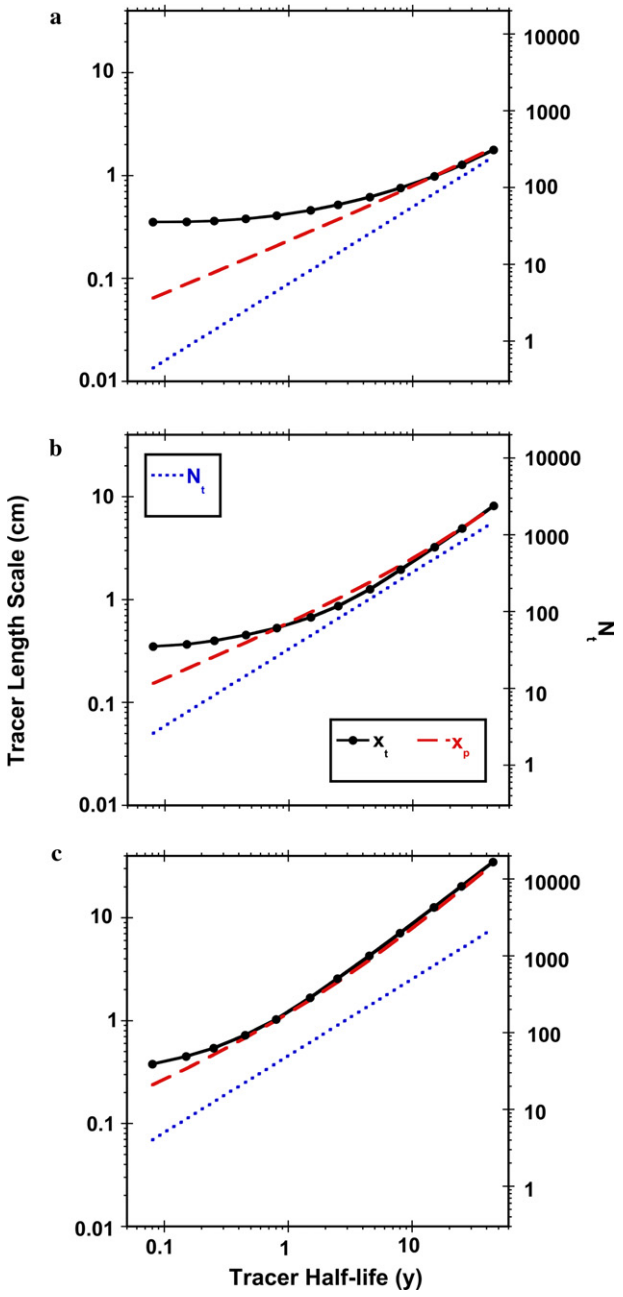

Fig. 4. The mean achieved tracer length scale (x_t; solid line), anticipated tracer length scale (x_p; dashed line), and average number of mixing events experienced by a radioisotope before decaying (N_t; dotted line) versus tracer half-life ($t_{1/2}$) for (a) abyssal, (b) slope and (c) coastal parameter sets.

x_t is larger than expected (i.e. x_p) when insufficient mixing events have been experienced (i.e. when N_t is too small). Fig. 2 illustrates how this translates into the observed dependence of D_b^t on tracer half-life. It is important to note, tracer profiles rarely provide any evidence that the model's assumptions have been violated in this way. Therefore, relying on tracer profiles alone, one could easily and erroneously surmise, owing to no indications of model breakdown, that the observed trend is real.

Field studies seem to provide support for this mechanism as the cause of the D_b^t–$t_{1/2}$ relationship. Employing transient tracers, Fornes et al. (1999, 2001) demonstrated that bioturbation appears nonlocal over short temporal scales, but becomes diffusive with time, in agreement with LABS simulations presented here. Fornes et al. (1999) also observed particle-selective mixing to a very limited degree, occurring only 30% of the time. Furthermore, the modes of selective particle transport encountered by Fornes et al. (2001) were typically nondiffusive, suggesting that particle-selectivity would only further contribute to violating the assumptions of the biodiffusion model.

6.3. Boundary conditions

Typically when applying the biodiffusion model, a semi-infinite mixed layer is assumed with a homogeneous Neumann boundary condition at the lower bound (i.e. $\lim_{x\to\infty}\frac{dC}{dx}=0$). This condition represents no diffusive flux (i.e. no bioturbation) at an infinite depth and conveniently reduces the model solution to a single term (Boudreau, 1997). In LABS, however, the mixed layer is finite, as the lower boundary is impenetrable to organisms. This only becomes problematic when the tracer penetrates deep enough to be "aware" of the boundary. In such a case, the required boundary condition is,

$$\left.\frac{dC}{dx}\right|_{\mathcal{L}}=0 \tag{22}$$

where $\mathcal{L}$ is the mixed layer depth. Consequently, a second exponential term appears in the solution to the biodiffusion model. This additional term grows in magnitude with increasing depth, in contrast with the original term that decays with depth. In a physical context, the extra term accounts for the tracer that is retained in the mixed layer due to the boundary, instead of being mixed down into the interval $[\mathcal{L},\infty]$. This "extraneous" tracer is redistributed throughout the mixed layer, resulting in steeper profiles. Therefore, fitting the standard model solution, which assumes a semi-infinite mixed layer, to a profile influenced by the presence of a lower boundary will result in an erroneously large calculated D_b^t value. Fig. 5 compares the model solution with the two boundary conditions for three different radioisotopes (^{228}Th, ^{210}Pb, ^{32}Si). Note that the two solutions do not differ for the shortest-lived of the isotopes (^{228}Th), as this tracer does not "feel" the base of the mixed layer; the solutions differ notably for the longest-lived tracer (^{32}Si), as the presence of the lower boundary becomes significant.

To demonstrate the effect of neglecting the lower boundary, the standard model solution is fitted to a profile generated with the two-term solution and D_b^t determined from this fit (Fig. 5). The parameters used to generate the profiles were $\mathcal{L}=10$ cm, $\omega=0.05$ cm y^{-1} and $D_b=0.5$ cm^2 y^{-1}. For ^{228}Th ($t_{1/2}=1.9$ y), the fitted model determined D_b^t to be 0.5 cm^2 y^{-1}, equal to the D_b used to generate the profile. However, the model fit for ^{210}Pb ($t_{1/2}=22.3$ y) furnished a

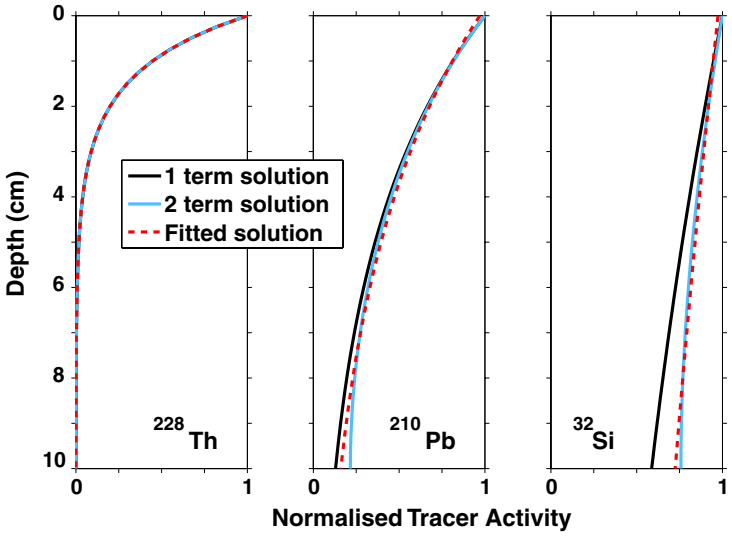

Fig. 5. The influence of a no diffusive flux lower boundary condition on tracer profiles. The solid black line represents the biodiffusion model solution with one term (semi-infinite mixed layer); the solid blue line represents the biodiffusion model solution with two terms (finite mixed later). $D_b = 0.5\ \mathrm{cm^2\ y^{-1}}$, $\omega = 0.05\ \mathrm{cm\ y^{-1}}$ and $\mathcal{L} = 10$ cm for both solutions. The dashed red line is the one term model solution fit to the calculated two term solution producing D_b values of 0.5, 0.7 and 3 $\mathrm{cm^2\ y^{-1}}$ for ^{228}Th ($t_{1/2} = 1.9$ y), ^{210}Pb ($t_{1/2} = 22.3$ y) and ^{32}Si ($t_{1/2} \approx 170$ y), respectively.

D_b^t of 0.7 $\mathrm{cm^2\ y^{-1}}$, while ^{32}Si ($t_{1/2} \approx 170$ y) gave a value of 3 $\mathrm{cm^2\ y^{-1}}$. Evidently, as the half-life of the tracer increases, so does the error in the calculated D_b^t. The larger the tracer half-life, the greater the amount of tracer retained and redistributed in the mixed layer. The consequence of this can be observed in LABS (Fig. 2c). When $t_{1/2}$ is suitably large so the penetration of the tracer is sufficiently deep to "feel" the mixed layer boundary, D_b^t rises with increasing tracer half-life. In nature, unlike LABS, there is no rigidly defined lower boundary and it is therefore likely that this effect is confined to our model. Increasing the depth of the mixed layer would remove this effect; however, due to the computationally expensive nature of LABS, the required increase in domain size is impractical.

In LABS, changing the mixed layer depth affects the mixing intensity by altering the rest period probability density function. Decreasing the mixed layer depth leads to more frequent particles displacements, i.e., τ becomes smaller due to the automatons being confined to a smaller region, and, in accordance with Eq. (15), the mixing intensity increases. Conversely, increasing the mixed layer depth results in less frequent particles displacements and, therefore, the mixing intensity decreases. The lower boundary also influences the mixing intensity by skewing the step length probability density function and increasing the step length variance. This is discussed further below.

6.4. Spatial dependence of D_b^p

Despite the automatons' burrowing rules having no dependence upon depth, some spatial variability is apparent in D_b^p values (Fig. 6). This variability is due to the presence of boundaries and is most notable at the

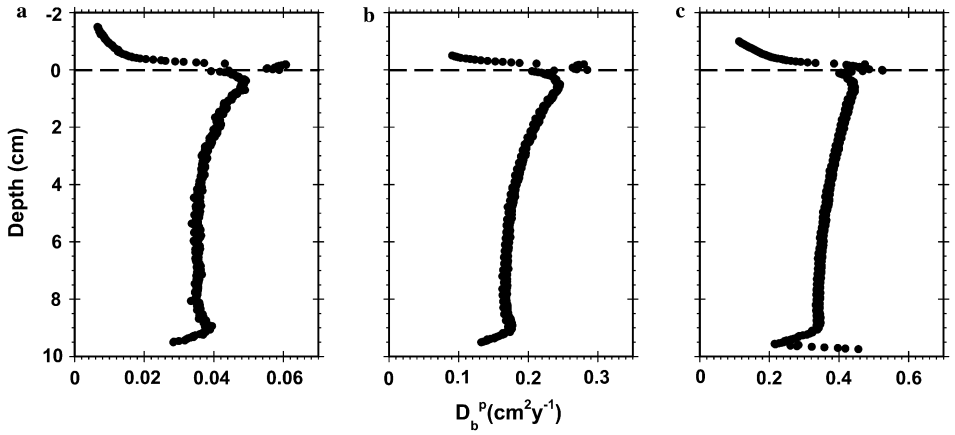

Fig. 6. The particle-tracking mixing coefficient (D_b^p) versus depth (x) for the (a) abyssal, (b) slope and (c) coastal parameter sets. The dashed line represents the original position of the sediment–water interface.

sediment–water interface—the effect of the lower boundary is relatively minor (e.g. Fig. 6b). In LABS, the base of the mixed layer is a static location in the lattice. In contrast, the sediment–water interface is a dynamic boundary influenced by automatons' activities, such as mound-building, and defined for the automatons with porosity based rules. The probability of automatons moving upwards is greatly reduced when the porosity reaches a certain threshold chosen to represent the sediment–water interface. Behaviour at the upper bound is, therefore, quite a complex issue. The distribution of particle displacements is skewed by the boundaries, increasing the variance of the step length distribution and thus the value of D_b^p (according to Eq. 15). Furthermore, asymmetry produces a nonzero mean displacement, which translates into a noticeable bioadvective drift (Eq. 14). Elsewhere in the mixed layer, there is a small background $\omega_b(x)$ due to compaction, which is typically negligible.

Observations of decreasing infaunal density with increasing distance from the sediment–water interface (e.g. Myers, 1977; Gambi and Bussotti, 1999; Glover et al., 2001) suggest that D_b should be a decreasing function of depth, although it is rarely treated this way (e.g. Christensen, 1982; Kadko and Heath, 1984; Boudreau, 1986a) as the functional form of D_b is not readily deducible from tracer profiles alone (Boudreau, 1986a). Christensen (1982) adopted a gaussian $D_b(x)$, reasoning that this form is appropriate due to the vertical distribution of fauna and nature of physical disturbances. Tracer profiles generated with a gaussian D_b were found to exhibit a flattening of the upper portion (Christensen, 1982), an effect that is present in LABS profiles from the slope simulation. When the constant D_b^t model is fit to such profiles, the resulting mixing coefficient underestimates the mixing that occurs. This is can be seen in Fig. 2b.

Imposing depth-dependent burrowing rules on the automatons produces depth dependent $D_b^p(x)$ functions of various forms. An example of such a rule is a linearly increasing reluctance to burrow deeper the farther the organism ventures into the sediment. This rule is perhaps representative of nature. The resulting $D_b^p(x)$ can be described well by a Gaussian function (Fig. 7). This demonstrates LABS' impressive ability to forge a direct link between animal behaviour and functional form of the mixing coefficient.

6.5. Failure of the biodiffusion model

It is important to note that violation of the biodiffusion model's criteria is rarely obvious in LABS tracer profiles. Researchers tend to rely on obvious indicators of nonlocal transport, such as subsurface maxima in radioisotope profiles, as evidence that the diffusion analogy is inappropriate. Subsurface maxima are likely to arise from the injection of surficial sediment at depth, perhaps due to "caching" feeding strategies (Jumars et al., 1990). However, this represents but one nonlocal mixing mode.

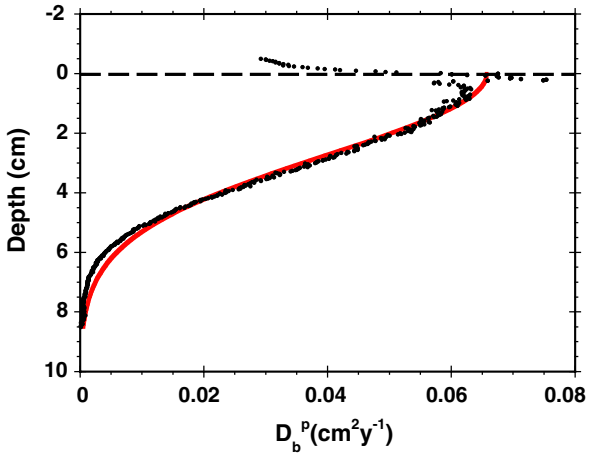

Fig. 7. The particle-tracking mixing coefficient (D_b^p) versus depth (x) for a simulation in which the automatons were prescribed depth-dependent burrowing rules. Specifically, the probability of the automatons burrowing deeper decreased linearly with increasing depth. The result is a $D_b^p(x)$ profile that is described well by a Gaussian function (solid line). The dashed line represents the original position of the sediment–water interface.

In contrast, if the direction of transport is reversed, so sediment is ingested at depth and defecated on to the sediment–water interface, i.e., conveyor-belt feeding (Rhoads, 1974), the resulting tracer profile does not possess a subsurface maxima and is indistinguishable from a diffusive profile despite particles being transported nonlocally (Boudreau, 1986b). The observation of "diffusive" profiles does not, therefore, provide evidence of local mixing.

Failure of the diffusion analogy is not restricted to short-lived radionuclides; subsurface maxima have been observed when using long-lived radioisotopes, such as ^{210}Pb (Smith et al., 1986; Soetaert et al., 1996). A more subtle manifestation of nonlocal mixing can be demonstrated by LABS. Using the abyssal parameter set with larger organisms, i.e., 5 cm, lengthwise, and a larger gut-to-body ratio of 0.5, the criteria underlying the biodiffusion model are violated for ^{210}Pb (Fig. 8). This increased gut-to-body ratio is quite realistic, as species of deep-sea deposit-feeding polychaetes have been observed to have larger gut-to-body ratios compared to their shallow water relatives, reaching values as large as 0.83 (Penry and Jumars, 1990). If this increased gut-to-body ratio translates into greater particle residence times in the gut, then particle displacement lengths increase accordingly. No subsurface maxima are apparent in the ^{210}Pb profiles. Instead, the tracer concentration decreases rapidly with depth to an asymptote (Fig. 8). Note that this profile is the excess (or unsupported) ^{210}Pb activity. Supported ^{210}Pb is usually relatively constant with depth, and the total ^{210}Pb profile would, therefore, be of the same form as Fig. 8, but shifted to the right. Presented with such a profile of total tracer activity, it would be tempting to incorrectly assume the value of the asymptote is the supported activity. This highlights the importance of measuring the supported component of tracer activity, as opposed to reckoning it from tracer profiles.

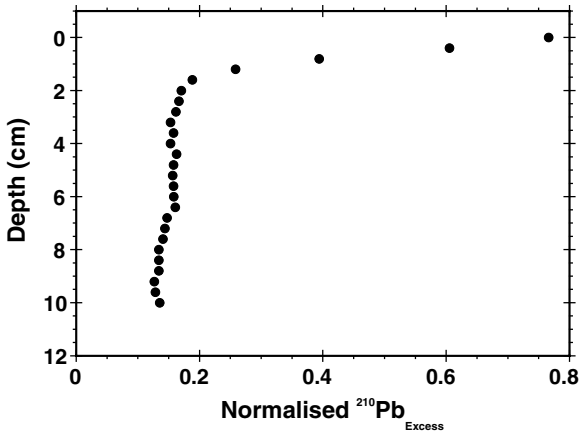

Fig. 8. A nonlocal ^{210}Pb profile from a simulation using the abyssal parameter set with organisms 5 cm in length and a gut-to-body ratio of 0.5. Tracer activity is normalised with the initial activity of a particle, i.e., new particles have unit activity. Accordingly, tracer activity is unitless.

Profiles such as Fig. 8 may prove misleading when interpreted in the context of diffusive mixing. For example, Fig. 8 could be described well by either a nonlocal model or, alternatively, a diffusion model with multiple mixed layers. Fitting the diffusion model with two mixed layers leads to the conclusion that the uppermost sediment is mixed at a much lower rate than the rest of the sediment, which is mixed at a very high rate. This is clearly incorrect. As discussed, D_b^p values show mixing is indeed *greatest* at the surface. In the case of Fig. 8, it is known from examining the model criteria that the diffusion model is inappropriate and a nonlocal model should be used.

However, in nature, evaluation of the biodiffusion model's criteria is not readily achievable and the appropriate model is not necessarily obvious. For example, Soetaert et al. (1996) demonstrated that profiles previously described by a multilayer diffusion model (Legeleux et al., 1994) can be described equally well by nonlocal models. Which model is most apt is not known. However, it seems more feasible for such profiles to be the result of a nonlocal mixing mechanism, such as that demonstrated by LABS, as opposed to a number of distinct mixing regimes confined to well-defined layers within the sediment. Furthermore, faunal activities tend to decrease with depth and physical disturbances occur in the uppermost sediment, suggesting this region should be the most intensely mixed. A multilayer diffusive model suggests the opposite (Legeleux et al., 1994). Ultimately, motivation for selecting a model of bioturbation should be derived from observations of the mediators and mixing mechanisms at work: goodness of fit does not provide justification alone.

Fig. 3 shows a decrease in the variability of D_b^t with tracer half-life. (Note that data affected by the artificial boundary conditions imposed by LABS, discussed above, are omitted from these plots for the sake of clarity.) Variability of D_b^t is a function of radionuclide half-life, as tracer half-life regulates the number of mixing events experienced by the tracer before decaying. As a result, a greater half-life provides a smoother time-averaged view of bioturbation. As the number of mixing events experienced before the tracer decays (i.e. N_t) increases, the variability of D_b^t decreases. However, there is a practical upperbound to the half-life used. Profiles of extremely long-lived radioisotopes, such as ^{14}C ($t_{1/2} = 5730$ y), may be homogeneous across the mixed layer (i.e. a vertical straight line), precluding the calculation of a D_b^t value. Therefore, a balance must be struck between having a suitably long enough half-life to give a good time-averaged D_b^t value and having a short enough half-life in order that the profile furnishes information on mixing.

7. Implications and conclusions

The biodiffusion model is the default description of biogenic reworking of sediments, with its validity rarely assessed. While it may initially be counterintuitive to think of bioturbation as a random, small scale, isotropic process, pleasing fits to field data seem to offer support to the model. However, as profiles produced by nonlocal mixing are often indistinguishable from those resulting from diffusive mixing, it is apparent that profiles provide little information regarding mixing mechanisms. Despite subsurface maxima in tracer profiles arising only from certain nonlocal mechanisms, they have been adopted as hallmarks of nonlocal mixing. Indeed, radioisotope profiles rarely exhibited subsurface maxima in LABS when the model criteria were violated. Results presented here echo conclusions drawn by previous studies (e.g. Meysman et al., 2003c) that the criteria of the biodiffusion model are usually violated for short-lived radioisotopes (i.e. ^{234}Th, ^{7}Be). It must be borne in mind that benthic organisms exist in a spectrum of sizes, both larger and smaller than the organisms modelled here. Also, the functional-group of organisms simulated represents the most likely candidates for diffusive mixing, in contrast to other agents of bioturbation that move sediment in a nonrandom fashion over large scales (i.e. comparable to the mixed layer depth), such as *Arenicola Marina*. An important conclusion of this study is that steady-state radioisotope tracers, especially short-lived tracers such as ^{234}Th, can *unknowingly* provide erroneous mixing coefficients. The results of (and conclusions drawn from) diagenetic models are reliant upon, among other factors, how well the processes they include are parameterised. Errors in D_b^t of the magnitude observed in LABS could radically alter the dynamics of models that include bioturbation as diffusive transport. For example, models describing chemical cycles that are heavily dependent upon bioturbation to supply (or remove) reactants (or products), such as models of iron, manganese and sulphur diagenesis. Furthermore, by violating the model's necessary criteria, trends can be fabricated (e.g. tracer-dependent mixing), leading to false conclusions being drawn. To be able to argue that such a trend is not actually an artifact of the biodiffusion model, it is necessary to verify that the model is indeed applicable. Field studies appear to

support the mechanism suggested here as the root of the D_b^t–$t_{1/2}$ relationship. In situ experimental work using transient tracers has demonstrated that bioturbation is not diffusive on short time scales, but only becomes diffusive over time (Fornes et al., 1999, 2001), in agreement with LABS simulations presented here. Furthermore, particle-selective mixing may be very limited (Fornes et al., 1999) and selective mixing mechanisms that exist are likely to be nondiffusive in nature (Fornes et al., 2001). These observations bolster the argument that short-lived tracers produce notably larger D_b^t values than longer-lived radioisotopes due to violation of the biodiffusion model's assumptions. Finally, interpreting nonlocal tracer profiles in the context of diffusive mixing can provide a misleading view of the rates, locations and mechanisms of bioturbation.

Acknowledgments

Financial support to B.P. Boudreau was provided by the US Office of Naval Research and the Natural Sciences and Engineering Research Council of Canada and to F.J.R. Meysman by a PIONIER grant (J.J. Middelburg, PI) from The Netherlands Organization for Scientific Research (NWO). The authors thank Dr. P.A. Jumars for providing valuable biological advice and the three journal reviewers for their useful comments.

Associate editor: John Crusius

References

Aller, R.C., 1982. The effects of macrobenthos on chemical properties of marine sediment and overlying water. In: McCall, P.L., Tevesz, M.J.S. (Eds.), *Animal-Sediment Interactions*. Plenum Publishing Corporation.

Aller, R.C., Rude, P.D., 1998. Complete oxidation of solid phase sulfides by manganese and bacteria in anoxic marine sediments. *Geochim. Cosmochim. Acta* **52** (2), 751–765.

Berger, W.H., Heath, G.R., 1968. Vertical mixing in pelagic sediments. *J. Mar. Res.* **26** (2), 134–143.

Berner, R.A., 1980. *Early Diagenesis: A Theoretical Approach*. Princeton University Press.

Bosworth, W.S., Thibodeaux, L.J., 1990. Bioturbation: a facilitator of contaminant transport in bed sediment. *Environ. Prog.* **9** (4), 211–217.

Boudreau, B.P., 1986a. Mathematics of tracer mixing in sediments: 1. Spatially-dependent, diffusive mixing. *Am. J. Sci.* **286**, 161–198.

Boudreau, B.P., 1986b. Mathematics of tracer mixing in sediments: 2. Nonlocal mixing and biological conveyor-belt phenomena. *Am. J. Sci.* **286**, 199–238.

Boudreau, B.P., 1994. Is burial velocity a master parameter of bioturbation? *Geochim. Cosmochim. Acta* **58** (4), 1243–1249.

Boudreau, B.P., 1996. A method-of-lines code for carbon and nutrient diagenesis in aquatic sediments. *Comput. Geosci.* **22** (5), 479–496.

Boudreau, B.P., 1997. *Diagenetic Models and their Implementation: Modelling Transport and Reactions in Aquatic Sediments*. Springer-Verlag.

Boudreau, B.P., Choi, J., Meysman, F.J.R., François-Carcaillet, F., 2001. Diffusion in a lattice-automaton model of bioturbation by small deposit-feeders. *J. Mar. Res.* **59**, 749–768.

Caron, A., Derosiers, G., Retière, C., Brenot, S., 1996. The behaviour of Nephtys caeca inside sediment under experimental conditions. *Comptes rendus de l' academie des sciences: Sciences de la vie* **319**, 417–423.

Choi, J., François-Carcaillet, F., Boudreau, B.P., 2002. Lattice-automaton bioturbation simulator (LABS): implementation for small deposit feeders. *Comput. Geosci.* **28** (2), 213–222.

Christensen, E.R., 1982. A model for radionuclides in sediments influenced by mixing and compaction. *J. Geophys. Res.* **87** (1), 566–572.

Cochran, J.K., 1985. Particle mixing rates in sediments of the eastern equatorial Pacific: evidence from ^{210}Pb, ^{239,240}Pu and ^{137}Cs distributions at MANOP sites. *Geochim. Cosmochim. Acta* **49**, 1195–1210.

Dorgan, K.M., Jumars, P.A., Johnson, B., Boudreau, B.P., Landis, E., 2005. Burrow extension by crack propagation. *Nature* **433**, 475.

Forbes, T.L. 1984. Aspects of the feeding biology of Capitella capitata Species 1: measurements of ingestion selectivity, egestion rate, and absorption efficiency. M.Phil. thesis, SUNY at Stoney Brook.

Fornes, W.L., DeMaster, D.J., Levin, L.A., Blair, N.E., 1999. Bioturbation and particle transport in Carolina slope sediments: a radiochemical approach. *J. Mar. Res.* **51**, 335–355.

Fornes, W.L., DeMaster, D.J., Smith, C.R., 2001. A particle introduction experiment in Santa Catalina Basin sediments: testing the age-dependent mixing hypothesis. *J. Mar. Res.* **59**, 97–112.

Gambi, M.C., Bussotti, S., 1999. Composition, abundance and stratification of soft-bottom macrobenthos from selected areas of the Ross Sea Shelf (Antarctica). *Polar Biol.* **21**, 347–354.

Glover, A., Paterson, G., Bett, B., Gage, J., Sibuet, M., Sheader, M., Hawkins, L., 2001. Patterns in polychaete abundance and diversity from Madeira Abyssal Plain, northeast Atlantic. *Deep-Sea Res. Pt. 1* **48**, 217–236.

Goldberg, E.D., Koide, M., 1962. Geochronological studies of deep sea sediments by the ionium/thorium method. *Geochim. Cosmochim. Acta* **26**, 417–450.

Grassle, J.F., Grassle, J.P., 1974. Opportunistic life histories and genetic systems in marine benthic polychaetes. *J. Mar. Res.* **32**, 253–284.

Grassle, J.P., Grassle, J.F., 1976. Sibling species in the marine pollutant indicator capitella (polychaeta). *Science* **192** (4239), 567–569.

Green, M.A., Aller, R.C., Cochran, J.K., Lee, C., Aller, J.Y., 2002. Bioturbation in shelf/slope sediments off Cape Hattera, North Carolina: the use of ^{234}Th, Chl-a, and Br^- to evaluate rates of particle and solute transport. *Deep-Sea Res. Pt. 2* **49**, 4627–4644.

Guinasso, N.L., Schink, D.R., 1975. Quantitative estimates of biological mixing rates in abyssal sediments. *J. Geophys. Res.* **80** (21), 3032–3043.

Hughes, B.D., 1995. Random walks and random environments. Vol. 1, Random walks, Clarendon Press.

Jumars, P.A., Mayers, L.M., Deming, J.W., Baross, J.A., Wheatcroft, R.A., 1990. Deep-sea deposit-feeding strategies suggested by environmental and feeding constraints. *Philos. Trans. R. Soc. London* **331**, 85–101.

Kadko, D., Heath, G.R., 1984. Models of depth-dependent bioturbation at Manop Site H in the Eastern Equatorial Pacific. *J. Geophys. Res.* **89** (C4), 6567–6570.

Legeleux, F., Reyss, J-L., Schmidt, S., 1994. Particle mixing rates in sediments of the northeast tropical atlantic: evidence from $^{210}Pb_{XS}$, ^{137}Cs, $^{228}Th_{XS}$ and $^{234}Th_{XS}$ downcore distributions. *Earth Planet. Sci. Lett.* **128**, 545–562.

Lopez, G., Levinton, J.S., 1987. Ecology of deposit-feeding animals in marine sediments. *Q. Rev. Biol.* **62** (3), 235–260.

Méndez, N., Linke-Gamenick, I., Forbes, V.E., Baird, D.J., 2001. Sediment processing in *Capitella* spp. (Polychaeta: Capitellidae): strain-specific differences and effects of the organic toxicant fluoranthene. *Mar. Biol.* **138**, 311–319.

Metzler, R., Klafter, J., 2000. The random walk's guide to anomalous diffusion: a fractional dynamics approach. *Phys. Rep.* **339**, 1–77.

Meysman, F.J.R., Middelburg, J.J., Herman, P.M.J., Heip, C.H.R., 2003a. Reactive transport in surface sediments. 1. Model complexity and software quality. *Comput. Geosci.* **29**, 291–300.

Meysman, F.J.R., Middelburg, J.J., Herman, P.M.J., Heip, C.H.R., 2003b. Reactive transport in surface sediments. 2. Media: an object-oriented proble,-solving environment for early diagenesis. *Comput. Geosci.* **29**, 301–318.

Meysman, F.J.R., Boudreau, B.P., Middelburg, J.J., 2003c. Relations between local, nonlocal, discrete and continuous models of bioturbation. *J. Mar. Res.* **61**, 391–410.

Middelburg, J.J., Soetaert, K., Herman, P.M.J., 1997. Empirical relationships for use in global diagenetic models. *Deep-Sea Res. Pt. 1* **44** (2), 327–344.

Myers, A.C., 1977. Sediment processing in a marine subtidal sandy bottom community: 2. Biological consequences. *J. Mar. Res.* **35** (3), 633–647.

Penry, D.L., Jumars, P.A., 1990. Gut architecture, digestive constraints and feeding ecology of deposit-feeding and carnivorous polychaetes. *Oecologia* **82**, 1–11.

Rhoads, D.C., 1974. Organism-sediment relations on the muddy sea floor. *Oceanogr. Mar. Biol.* **12**, 263–300.

Richter, R., 1952. Fluidal-texture in sediment-gesteinen und ober sedifluktion berhaupt. *Notizbl Hess Landesamtes Bodenforsch Wiesbaden* **3**, 67–81.

Smith, C.R., Pope, R.H., DeMaster, D.J., Magaard, L., 1993. Age-dependent mixing of deep-sea sediments. *Geochim. Cosmochim. Acta* **57**, 1473–1488.

Smith, C.R., Berelson, W., DeMaster, D.J., Dobbs, F.C., Hammond, D., Hoover, D.J., Pope, R.H., Stephens, M., 1997. Latitudinal variations in benthic processes in the abyssal equatorial pacific: control by biogenic particle flux. *Deep-Sea Res. Pt. 2* **44** (9–10), 2295–2317.

Smith, J.N., Boudreau, B.P., Noshkin, V., 1986. Plutonium and ^{210}Pb distributions in northeast Atlantic sediments: subsurface anomalies caused by non-local mixing. *Earth Planet. Sci. Lett.* **81**, 15–28.

Soetaert, K., Herman, P.M.J., Middelburg, J.J., Heip, C., deStigter, H.S., vanWeering, T.C.E., Epping, E., Helder, W., 1996. Modeling ^{210}Pb-derived mixing activity in ocean margin sediments: diffusive versus nonlocal mixing. *J. Mar. Res.* **54**, 1207–1227.

Stordal, M.C., Johnson, J.W., Guinasso, N.L., Schink, D.R., 1985. Quantitative evalulation of bioturbation rates in deep ocean sediments. 2. Comparison of rates determined by ^{210}Pb and ^{239,240}Pu. *Mar. Chem.* **17**, 99–114.

Turnewitsch, R., Witte, U., Graf, G., 2000. Bioturbation in the abyssal arabian sea: influence of fauna and food supply. *Deep-Sea Res. Pt. 2* **47**, 2877–2911.

Wheatcroft, R.A., Jumars, P.A., Smith, C.R., Nowell, A.R.M., 1990. A mechanistic view of the particulate biodiffusion coefficient: step lengths, rest periods and transport directions. *J. Mar. Res.* **48**, 177–207.

Yingst, J.Y., Rhoads, D.C., 1978. Seafloor stability in central long island sound: part 2. biological interactions and their potential importance for seafloor erodibility. In: Wiley, M. (Ed.), *Estuarine Interactions*. Academic Press, Inc.